RSC Advances

Journal Name

ARTICLE

Received 00th January 20xx,
Accepted 00th January 20xx

DOI: 10.1039/x0xx00000x

Ultrasound accelerated sugar based gel for *in situ* construction of Eu^{3+}-based metallogel via energy transfer in supramolecular scaffold

Tao Wang, Zengyao Wang, Dongyan Xie, Chong Wang, Xiaoli Zhen, Yajuan Li *, Xudong Yu*

Abstract. Two sugar functionalized naphthalimide derivatives (**S1**, **S2**) self-assembled into organogels by heating-cooling process or triggered by ultrasound. The gelation properties of them in organic solvents were examined by several experiments including UV-vis, Fluorescence, FT-IR spectra and SEM, XRD techniques. It was deduced that minor changes in the terminal group had great impact on the gelation and ultrasound responsive properties. Moreover, ultrasound triggered the formation of yellow emissive gel (**S1**, with lifetimes in the range of ns) that was readily doped with Eu^{3+} *in situ* affording luminescent gels with red emission color (with lifetimes in the range of μs), which expressed the efficient energy transfer from **S1** assembly to Eu^{3+} ion. It was presented that the efficient energy transfer only happened in the ordered fibrous aggregates of **S1**, whereas, the ET process was not observed in solution state, indicating the phase control on the ET process. Such finding would pave a new way for the construction of novel rare earth based luminescent materials.

Introduction

Excitation energy transfer (ET) in nanostructured material has attracted increasing interest due to its applications in OLEDs, photonics and light-harvesting systems.[1-8] Recently, much attention has been focused on the ET process in highly organized, supramolecular assembly of donor-acceptor system.[9-10] In an ordered assembly material such as crystals, polymers and nanoparticles, they often displays highly efficient energy transfer.[11-12] Assembly of them could also lead to solvent trapping and formation of functional organogels through non-covalent interactions.[13-28] Self-organization of chromophores in gel tissues often results in the precise and homogeneous arrangement of them which facilitate the energy transfer process and tuning the emission colors.[29-30] Even though great efforts have been performed in construction of optical supramolecular assemblies controlled by energy transfer, the control on the metal based ET process in gel network has scarecely been concerned, which are of primary importance for optoelectronic applications and biologically light-harvesting devices.

Lanthanide complexes especially Eu^{3+} or Tb^{3+} complexes possess desirable and unique photophysical properties.[31-35] The generally accept mechanism of them is the energy transfer from the energy matching ligand to the lanthanide ion, which is called antenna effects. β-diketonates, aromatic carboxylates and heterocyclic ligands are found to be efficient sensitizers for lanthanide ions in either solution or solid state. Recently, T. Gunnlaugsson and M. H. Liu et al reported that doping lanthanide ions in gel networks would generate higher luminescent properties compared with that of solution.[36-37] Also, N. Holten-Andersen and coworkers studied the white emitting lanthanide metallogels with tunable luminescence.[38] Such strategy would provide a pathway for construction of new types of optical luminescent metallogels based on ET process.[39] However, design of novel paradigms showing the necessary of the luminescence of lanthanide ions in gel scaffold remains elusive because that the energy transfer from ligand to lanthanide ion often happens in both solution and gel state. Phase control on the ET process via “off-on” approach would open a new method for constructing stimulus gated optical devices.

In previous works, we reported a series of 4-amino-naphthalimide derivatives, which could form organogels or hydrogels with yellow/green emission colors. We also studied their applications in the field of sensors and drug release system.[40-46] Herein, to extend our works, we showed that the well-organized naphthalimide-based aggregates accelerated by ultrasound in gel networks could also serve as efficient energy donor for Eu^{3+} ion, and such energy transfer enabled the *in situ* construction of red-emission-color metallogel resulted from yellow-green organogel (Scheme 1, Fig. 1). Whereas, The ET

Hebei Research Center of Pharmaceutical and Chemical Engineering, and College of Science, Yuhua Road 70, Shijiazhuang 050080, PR China
† Electronic Supplementary Information (ESI) available: [details of experiment section, additional spectra and images]. See DOI: 10.1039/x0xx00000x
‡Joint first authors contributed equally to this work

process was not observed in the solution state. The contrast with stacked gel system, where nanofibrils as a linear path were expected for the efficient energy transfer, and was believed to favorably design novel materials for optical information transfer. To the best of our knowledge, this is the first to describe how the ET process could happen from 4-amino-naphthalimide derivative to rare earth ions.

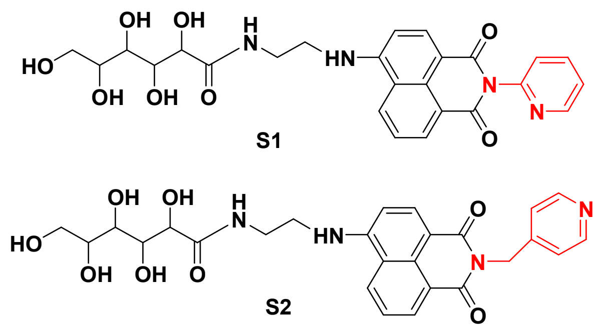

Scheme 1 The chemical structures of **S1** and **S2**.

Experiment

Materials

All starting materials were obtained from commercial supplies and used without further purification. δ-Gluconolactone was provided from Alfa Aesar. 4-Bromo-1, 8-naphthalic anhydride (95%), Ethylenediamine, 4-picolylamine, 2-(Methylamino) Pyridine, and other reagents were supplied from Shanghai Darui fine chemical Co. Ltd. All the solvents used for gelation test were dried to remove water. For example, ethanol were dried by Ma and I_2 in refluxed state, and the water content was < 0.05%.

Techniques

FTIR spectra were recorded by using an IRPRESTIGE-21 spectrometer (Shimadzu). SEM images of the xerogels were obtained by using SSX-550 (Shimadzu) and FE-SEM S-4800 (Hitachi) instruments. Samples were prepared by spinning the gels on glass slides and coating them with Au. NMR spectra were performed on a Bruker Advance DRX 400 spectrometer operating at 500/400 and 125/100 MHz for ^{1}HNMR and ^{13}CNMR spectroscopy, respectively. The high-resolution mass spectra (HR-MS) were measured on a Bruker Micro TOF II 10257 instrument. Fluorescence spectra were collected on an Edinburgh instrument FLS-920 spectrometer with a Xe lamp as an excitation source. The X-ray diffraction pattern (XRD) was generated by using a Bruker AXS D8 instrument (Cu target; λ = 0.1542 nm) with a power of 40 kV and 50 mA. UV-Vis absorption spectra were recorded on a UV-vis 2550 spectroscope (Shimadzu). Sonication treatment of a sol was performed in a KQ-500DB ultrasonic cleaner (maximum power, 100 W, 40 KHz, Kunshan Ultrasound Instrument Co, Ltd., China).

Results and discussion

The synthesis and characterization of **S1** and **S2** could be seen from ESI. Upon dissolving **S1** in ethanol with sonication for seconds, a fluorescent organogel which was called S-gel formed immediately (Scheme 1). Whilst, **S2** was able to gel in ethyl acetate by classic heating-cooling process (the gel was called T-gel, Fig. 2). The UV-Vis absorption and emission properties of **S1** and **S2** both in solution and gel state could be shown in Fig. 3. Both the solution (10^{-4} M) and S-gel of **S1** (25 mg/mL) showed the same maximum absorption peaks at 436 nm, which were attributed to the ICT process of 4-amino-naphthalimide. In the fluorescence spectra, **S1** in the solution displayed the emission peak at 523 nm, 25 nm red shift was observed in the S-gel compared with that of solution, indicating the aggregation-induced emission changes. Similar fluorescent spectrum changes were also found in the gel of **S2** (Fig. S1a). The UV-Vis spectra of **S2** T-gel banded at 436 nm showed 9 nm blue shift from the solution, revealing the H aggregate of naphthalimide segments (Fig. S1b).

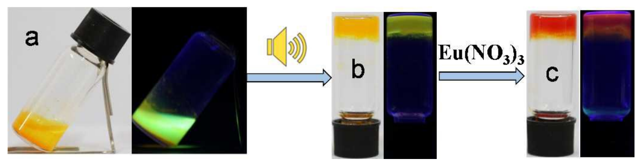

Fig. 1 illustration of ultrasound triggered gelation of **S1** for *in situ* construction of metallogel with red color emission.

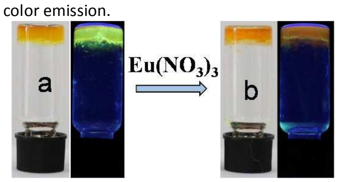

Fig. 2 illustration of T-gel of **S2** and the gel when doped with $Eu(NO_3)_3$ ions.

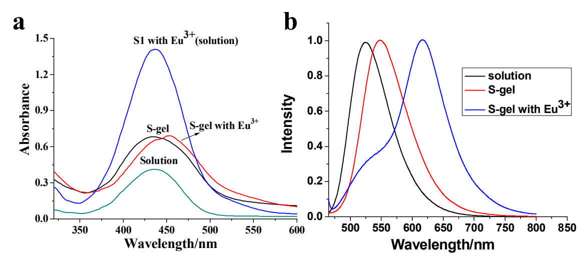

Fig. 3 a) UV-vis spectra of **S1** solution (10^{-4} M), **S1** solution with Eu^{3+} (20 eq.), **S1** gel (25 mg/mL), and **S1** S-gel (25 mg/mL) with Eu^{3+} (100 mg/mL); b) the corresponding fluorescence spectra.

The macrostructure information could be reflected by the SEM images. Seen from Fig. S2, by a heating-cooling process, **S1** (25 mg/mL) precipitated from ethanol with irregular nanoparticle morphology. While the S-gel showed folded sheet structure, which was produced by the cavity effect of ultrasound (Fig. 3a, 3b).[39] With different structure in the terminal group, **S2** organogel consisted of entangled and dense nanofibrils that were about 25 nm in width (Fig. 3d, 3e). Hydrogen bonding was essential for the gelation process. Both the precipitate and S-xerogel of **S1** showed -NH/-OH vibrations at 3401 cm^{-1} and –C=O vibrations at 1636 and 1580 cm^{-1} (Fig. S3). The T-xerogel of **S2** from ethyl acetate displayed weaker intermolecular hydrogen bonding strength compared with that of **S1** (Fig. S4, with -NH/-OH vibrations at 3425 cm^{-1}). XRD data revealed the different aggregation modes of precipitate and S-gel of **S1** (Fig. S5). However, we failed to find more information about the aggregation pattern. From the above results, it was deduced that the morphological change and long-range order of molecular assembly were responsible for the sonication triggered gelation. Temperature dependent fluorescence of **S1** S-gel could be seen in Fig. S6, upon heating the gel to a suspension from 25 °C to 60 °C, the maximum peak of S-gel at 548 nm displayed 12 nm red shift gradually, together with fluorescence quenching by a factor of 3.5, indicating the π-π stacking interactions among the naphthalimide groups. The above results suggested that the delicate balance of hydrogen bonding, π-π stacking interactions and hydrophilic interaction was responsible for the gelation properties of both **S1** and **S2**.

Pyridine and carbonyl segments have served as good coordination sites for lanthanide ions. The simple mixture of **S1** or **S2** and Eu^{3+} (with different ratios) could not form gels either by heating-cooling process or sonication treatment. Interestingly, when doping the Eu^{3+} ion on the fresh gel surface, and then staying for hours, red emission color gels could be obtained. Fig. 5 showed the gradual emission color changes of **S1** S-gel upon the addition of Eu^{3+} ion. The concentration range of $Eu(NO)_3$ from 2.5 mg/mL to 100 mg/mL doped in the gels (25 mg/mL) was all in favor of the red emission color metallogel and the complete gel-to-gel transition time with full color emission could be easily tuned from 40 min to 160 min (Table S2, Fig. 7, Fig. S7a). When $Eu(NO)_3$ was too less, no obvious changes could be observed. For example, upon addition of 0.5mg $Eu(NO_3)_3$ on the gel surface (25 mg/mL), no obvious fluorescence changes were observed compared with that of the original S-gel (Fig. S7b).

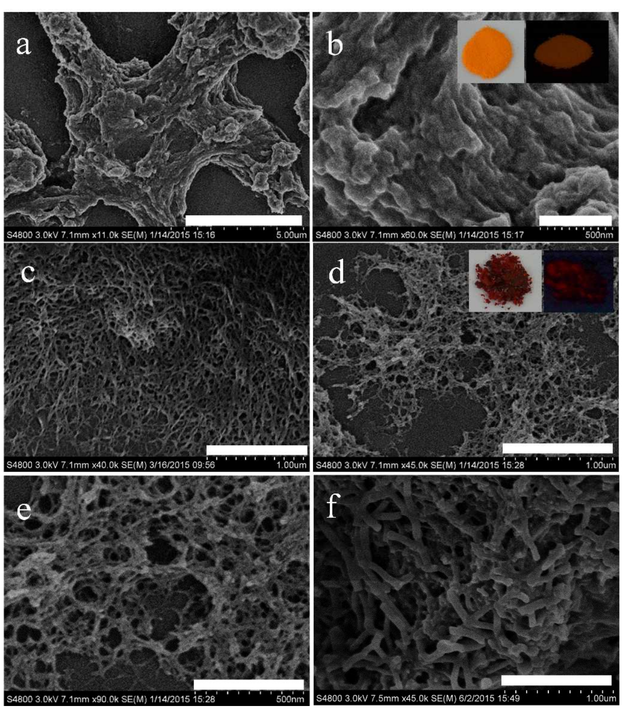

Fig. 4 SEM images of **S1** and **S2** assembly. a) S-xerogel of **S1** (25 mg/mL) from ethanol; b) was magnification picture of a); insert picture: photos of S-xerogel of **S1**; c) T-xerogel of **S2** from ethyl acetate; d) Xerogel of **S1** S-gel (5 mg/200 μL) doped with $Eu(NO_3)_3$ ion (10 mg); e) magnification picture of d); f) Xerogel of **S2** gel doped with $EuCl_3$ ion (10 mg). Scale bar: a) 5 μm; b) 500 nm; c) 1 μm; d) 1μm; e) 500 nm; f) 1μm.

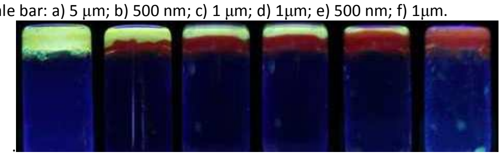

Fig. 5 Photos of **S1** S-gel after doping $Eu(NO)_3$ ions (in dark irradiated by 365 nm). From left to right: **S1** S-gel (5 mg/200 μL); upon the addition of $EuCl_3$ (10 mg) and then after staying for some time. From left to right: 8 min, after 13 min, after 20 min, after 40 min, and after 55 min.

IR spectra was employed to study the binding event of **S1** S-gel assembly with Eu^{3+} ion. Seen from Fig. 6, when the S-gel was coated with Eu^{3+}, the C=O vibration of **S1** S-xerogel banded at 1541 cm^{-1} changed to 1551 cm^{-1}. Simultaneously, the peaks at 1367, 1398 cm^{-1}, which belonged to stretching bands of pyridine group, moved to 1352 and 1385 cm^{-1}, also, the bending band of pyridine group at 772 cm^{-1} shifted to 775 cm^{-1}. The above results certified the coordination interaction between **S1** assembly and Eu^{3+} ions. SEM images also reflected the same result. The folded sheet structure of **S1** S-gel (25 mg/mL) was transformed into fibrous networks upon the addition of Eu^{3+} (50 mg/mL), indicating that Eu^{3+} was penetrated into the gel networks through coordination interaction (Fig. 3a, 3b, 3c). On the other hand, the nanofibrils of **S2** T-gel became thicker than that of the original state when **S2** aggregates were coordinated with Eu^{3+} ions. Such difference between the gel-to-gel transitions of **S1** and **S2** induced by Eu^{3+} ions might be attributed to the different coordination spaces of **S1** and **S2**. The results presented that 1D nanofibrils as a linear path was favorable for the co-assembly of gel aggregates with Eu^{3+} ions and the efficient energy transfer, which did not happen in the diluted solution state.

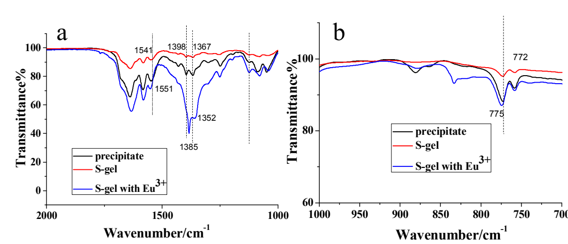

Fig. 6 IR spectra of **S1** precipitate from ethanol, S-xerogel and S-xerogel with Eu^{3+} from ethanol.

Fluorescent experiments were carried out to investigate the optical properties of the obtained metallogels and energy transfer process between naphthalimide-pyridine segment as energy donor and Eu^{3+} ion as energy acceptor in supramolecular gel scaffold. Upon the addition of 10 mg $Eu(NO_3)_3$, the peak of **S1** S-gel (25 mg/mL) at 548 nm decreased obviously by a factor of 2.7, and a new peak at 618 nm appeared, corresponding to the $5D^0 \rightarrow 7F^2$ transition of Eu^{3+} emission peak (Fig. 1).[36] Seen from Fig. 7 and S7, the emission peaks of the resulted metallogels with different amount of $Eu(NO_3)_3$ shifted from 600 nm to 618 nm, which displayed 50-70 nm red shift compared with that of the S-gel. The shoulders at 519 nm were ascribed to weaker ICT process of 4-amino-naphthalimide in the metallogels, clearly demonstrating the efficient energy transfer from naphthalimide-pyridine group to Eu^{3+} ion, and the weakened ICT process of 4-amino-naphthalimide segments. The energy transfer between **S2** T-gel assembly and Eu^{3+} appeared to be less efficient than that of **S1** (Fig. S1a, the peak of **S2** T-gel with Eu^{3+} in fluorescent spectrum was positioned at 560 nm). One of the reasons was that the rotation of the linker of CH_2 segment between naphthalimide and pyridine groups would result in the energy dissipation. The fluorescence spectra of the solid were also studied. The S-xerogel of **S1** displayed 34 nm red shift compared with that of gel state, similar fluorescence spectrum changes could be also observed in our recent study[47]. The peak of **S1** S-xerogel with Eu^{3+} (2.5 mg/mL) red shifted from 600 to 618 nm compared with that of S-gel with Eu^{3+}, which was ascribed to the $5D_0 \rightarrow 7F_2$ transition of Eu^{3+} emission peak, and reflected a more efficient energy transfer from **S1** assembly to Eu^{3+} ions (Fig. S8).

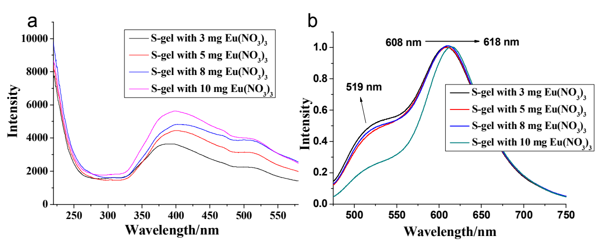

Fig. 7 Excitation and emission spectra of **S1** S-gel (5 mg/200 μL) with different amount of Eu^{3+}.

The lifetime values of the gels and solutions can be determined by the luminescent decay curves. As seen from Fig. 8a, the lifetimes of **S1** solution and **S1** solution with Eu^{3+} were determined to 8.7 ns and 7.7 ns respectively, indicating that almost no energy transfer happened between **S1** and Eu^{3+} in the solution state and only **S1** emitted. Whist, in the gel state, the lifetimes of the resulted metallogels were in the range from 12 to 16 μs, which was much longer than that of S-gel (with lifetime of 1.6 ns,Table S3). These features suggested that in the gel networks, the Eu^{3+} ions were in a more rigid environment, clearly confirming the tight bond between **S1** aggregates and Eu^{3+} ions.

Temperature dependent fluorescence was carried out to examine the thermal stability of the metallogel (5 mg/200 μL of **S1** with 10 mg $Eu(NO_3)_3$). By heating the gel from 25 °C to 80 °C with gel-to-suspension transformation, the emission peaks of Eu^{3+} ions expressed red shift from 618 nm to 627 nm, and the shoulder at 519 nm disappeared, indicating a more efficient energy transfer at higher temperature (Fig. S9).

To further confirm the necessary of the gel assembly for the energy transfer process, the metallogel aggregates (S-gel of **S1** with 10 mg Eu^{3+}) was diluted gradually in to solution states with concentration range from 5×10^{-3} M to 1×10^{-6} M, and emission peaks gradually blue-shifted from 531 nm to 517 nm, reflecting no Eu^{3+} emission peaks in the solution state (Fig. 9).

From the above results, our works can be summarized as following (Fig. 10): In the solution state, single molecule of **S1** existed, which did not assist the energy transfer from naphthalimide to Eu^{3+} ion because that the energy level of **S1** ligand did not match with Eu^{3+} ion, and the high frequency vibration of –OH of ethanol molecule among Eu^{3+} ions was also not favorable for the Eu^{3+} emission. In a gel state, the reasons for the efficient energy transfer can be attributed to three points: 1) the long-range organization of **S1** or **S2** molecules directed the ordered co-assembly of Eu^{3+} ions and the molecular aggregates, and a good dispersion could facilitate the energy transfer; 2) the molecular rotations were restricted in gel tissues, thus reducing the energy dissipation; 3) the **S1** molecular assembly constructed by non-covalent interactions behaved as a kind of supramolecular polymer, which supplied multiple coordination sites toward Eu^{3+} ions, and kept Eu^{3+} ions away from solvent molecules, finally resulting in the efficient energy transfer.

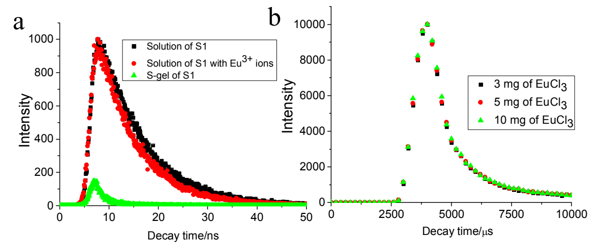

Fig. 8 Fluorescence decay profiles of **S1** and **S1** with $Eu(NO)_3$ in different states. a) Fluorescence decay profiles of **S1** solution (10^{-4} M), solution of **S1** (10^{-4} M) with Eu^{3+} ion (20 eq.), S-gel of **S1** (25 mg/mL); b) Fluorescence decay profiles of S-gel (5 mg/200 μL) with Eu^{3+} ions.

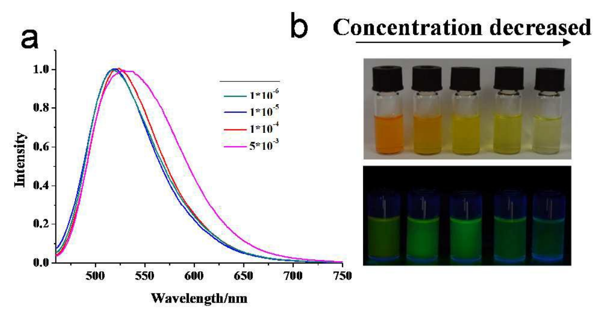

Fig. 9 a) the fluorescent spectra of **S1** solutions with Eu^{3+} when the metallogel was diluted gradually.

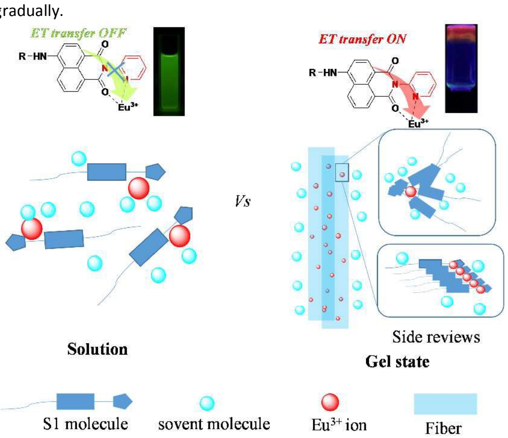

Fig. 10 illustration of the assembly mechanism and energy transfer process of S1 and Eu^{3+} ions.

Conclusions

In brief, two new kind of sugar based organogelators were designed and characterized. Tiny variation in the terminal group had great influence on the gelation properties and optical properties. Efficient excited energy transfer from 4-amino-naphthalimide chromophore to Eu^{3+} ion had been achieved in bulk organogels for the first time. In this context, we demonstrated that creation of high ordered assembly of nanofibril was important when the energy transfer process was addressed. Even though a significant amount of works have been focused on the energy transfer in gel networks, control of energy transfer between ligands and ions in nanoscale still remains a challenge. Therefore, this work would pave a new strategy to construct optical materials especially Lanthanide based nanodevices.

Acknowledgements

The authors thanks for the financial support by NNSFC (21401040, 21301047), Xiaoli fund SW (2014PT76), Natural Science Foundation of Hebei Province (No.B2014208160, B2014208091).

Notes and references

1 M. Bälter, M. Hammarson, P. Remón, S. Li and N. Gale, T. Brown, J. Andréasson, *J. Am. Chem. Soc.* 2015, **137**, 2444.
2 Freek J. M. Hoeben, A. P. H. J. Schenning and E. W. Meijer, *ChemPhysChem*, 2005, **6**, 2337..
3 E. Vaganova, E. Wachtel, G. Leitus, D. Danovich, S. Lesnichin, L. G. Shenderovich, H. Limbach and S. Yitzchaik, *J. Phys. Chem. B* 2010, **114**, 10728.
4 H. Dong, L. Sun and C. H. Yan, *Chem. Soc. Rev.*, 2015, **44**, 1608.
5 C. E. Rowland, I. Fedin, H. Zhang, S. K. Gray, A. O. Govorov, D. V. Talapin and R. D. Schaller, *Nat Mater*, 2015, **14**, 484.
6 T. H. Noh, H. Lee, J. Jang and O. Jung, *Angew. Chem. Int. Ed.,* 2015, **54**, 9284.
7 H. Peng, L. Niu, Y. Chen, L. Wu, C. Tung and Q. Yang, *Chem. Rev.,* 2015, **115**, 7502.
8 I. Moreels, *Nat Mater*, 2015, *14*, 464.
9 A. Ajayaghosh, V. K. Praveen and C. Vijayakumar, *Chem. Soc. Rev.,* 2008, **37**, 109.
10 P. Xue, R. Lu, P. Zhang, J. Jia, Q. Xu, T. Zhang, M. Takafuji and H. Ihara, *Langmuir* 2013, 29, 417.
11 A. Guerzo, A. G. L. Olive, J. Reichwagen, H. Hopf and J. Desvergne, *J. Am. Chem. Soc.,* 2005, **127**, 17984.
12 J. Wu, Q. Tian, H. Hu, Q. Xia, Y. Zou, F. Li, T. Yi and C. Huang, *Chem. Commun.,* 2009, 4100.
13 X. Cao, L. Y. Meng, Z. H. Li, Y. Y. Mao, H. C. Lan, L. M. Che, Y. Fan and T. Yi, *Langmuir* 2014, **30**, 11753.
14 X. Cao, A. Gao, H. Lv, H. Lan, Q. Cheng and N. Zhao, *RSC Adv.*, 2015, **5**, 48500.
15 S. S. Babu, V. K. Praveen and A. Ajayaghosh, *Chem. Rev.,* 2014, **114**, 1973.
16 N. Yan, Z. Y. Xu, K. K. Diehn, S. R. Raghavan, Y. Fang and R. G. Weiss, *J. Am. Chem. Soc.,* 2013, **135**, 8989.
17 C. Yu, M. Xue, K. Liu, G. Wang and Y. Fang, *Langmuir* 2014, **30**, 1257.
18 Y. Zhang, H. Ding, Y. F. Wu, C. X. Zhang, B. L. Bai, H. T. Wang and M. Li, *Soft Matter*, 2014, **10**, 8838.
19 X. Zhang, S. Y. Lee, Y. F. Liu, M. J. Lee, J. Yin, J. L. Sessler and J. Y. Yoon, *Sci. Rep.,* 2014, **4**, 4593.
20 J. R. Hiscock, M. R. Sambrook, N. Wells and P. A. Gale, *Chem. Sci.,* 2015,**6**, 5680.
21 S. Datta and S. Bhattacharya, *Chem. Soc. Rev.,* 2015, **44**, 5596.
22 K. Lalitha and S. Nagarajan, *J. Mater. Chem. B,* 2015, **3**, 5690.
23 J. F. Galisteo-López, S. Gómez-Esteban, B. Gómez-Lor and C. López, *J. Mater. Chem. C,* 2015, **3**, 5764.
24 B. N. Ghosh, S. Bhowmik, P. Mal and K. Rissanen, *Chem. Commun.*, 2014, **50**, 734.
25 Z. Li, Y. Su, B. Xie, X. Liu, X. Gao and D. Wang, *J. Mater. Chem. B,* 2015, **3**, 1769.
26 R. Mateen and T. Hoare, *J. Mater. Chem. B,* 2014, **2**, 5157.
27 J. Zhou, X. Du, J. Li, N. Yamagata and B. Xu, *J. Am. Chem. Soc.*, 2015, **137**, 10040.
28 X. Cao, Y. Wu, K. Liu, X. Yu, B. Wu, H. Wu, Z. Gong and Tao Yi, *J. Mater. Chem.,* 2012, **22**, 2650.
29 T. Shu, J. Wu, M. Lu, L. Chen, T. Yi, F. Li and C. Huang, *J. Mater. Chem.,* 2008, **18**, 886.
30 S. V. Eliseevaa and J. G. Bünzli, *Chem. Soc. Rev.*, 2010, **39**, 189.
31 B. Yan, *RSC Adv.*, 2012, **2**, 9304.
32 J. Feng and H. Zhang, *Chem. Soc. Rev.*, 2013, **42**, 387.
33 J. Zhao, Z. Wei, X. Feng, M. Miao, L. Sun, S. Cao, L. Shi and J. Fang, *ACS Appl. Mater. Interfaces*, 2014, **6**, 14945.
34 M. Shang, G. Li, X. Kang, D. Yang, D. Geng and J. Lin, *ACS Appl. Mater. Interfaces*, 2011, **3**, 2738.
35 Y. Li and B. Yan, *J. Mater. Chem.*, 2011, **21**, 8129.
36 M. Martínez-Calvo, O. Kotova, M. E. Möbius, A. P. Bell, T. McCabe, J. J. Boland and T. Gunnlaugsson, *J. Am. Chem. Soc.* 2015, **137**, 1983.
37 Y. Liu, T. Wang and M. H. Liu, *Chem. Eur. J.* 2012, **18**, 14650.
38 P. Chen, Q. Li, S. Grindy and N. Holten-Andersen, *J. Am. Chem. Soc.,* 2015, DOI: 10.1021/jacs.5b07394.
39 S. K. M. Nalluri and R. V. Ulijn, *Chem. Sci.,* 2013, **4**, 3699.
40 X. D. Yu, L. M. Chen, M. M. Zhang and T, Yi, *Chem. Soc. Rev.,* 2014, **43**, 5346.
41 X. L. Pang, X. D. Yu, H. C. Lan, X. T. Ge, Y. J. Li, X. L. Zhen and T. Yi, *ACS Appl. Mater. Interfaces,* 2015, **7**, 13569.
42 X. D. Yu, P. Zhang, Y. J. Li, L. M. Chen, T. Yi and Z. C. Ma, *Cryst EngComm,* 2015, **17**, 8039.
43 Z. C. Ma, P. Zhang, X. D. Yu, H. C. Lan, Y. J. Li, D. Y. Xie, J. Y. Li and T. Yi, *J. Mater. Chem. B,* 2015, 3, 7366.
44 X. Yu, Q. Liu, J. Wu, M. Zhang, X. Cao, S. Zhang, Q. Wang, L. Chen and T. Yi, *Chem. Eur. J.,* 2010, **16**, 9099.
45 L. Geng, Y. Li, Z. Wang, Y. Wang, G. Feng, X. Pang and X. D. Yu, *Soft Matter*, 2015, **11**, 8100.
46 X. D. Yu, X. Cao, L. Chen, H. Lan, B. Liu and T. Yi, *Soft Matter,* 2012, **8**, 3329.
47 X. D. Yu, X. T. Ge, H. C Lan, Y. J. Li, L. J. Geng, X. L. Zhen, and T. Yi, ACS Appl. Mater. Interfaces 2015, **7**, 24312.

TOC

Phase control on the energy transfer process via “off-on” approach between 4-amino-naphthalimide derivative and Eu^{3+} ion was achieved in sugar-based organogel tissue.